Stem Cell Reports
Article

OPEN ACCESS

Generation and Analysis of *GATA2*$^{w/eGFP}$ Human ESCs Reveal ITGB3/CD61 as a Reliable Marker for Defining Hemogenic Endothelial Cells during Hematopoiesis

Ke Huang,[1,2,5] Jiao Gao,[3,5] Juan Du,[1,2,5] Ning Ma,[1,2] Yanling Zhu,[1,2] Pengfei Wu,[1,2] Tian Zhang,[1,2] Wenqian Wang,[4] Yuhang Li,[1,2] Qianyu Chen,[1,2] Andrew Paul Hutchins,[1,2] Zhongzhou Yang,[1,2] Yi Zheng,[1,2] Jian Zhang,[1,2] Yongli Shan,[1,2] Xuejia Li,[1,2] Baojian Liao,[1,2] Jiajun Liu,[4] Jinyong Wang,[1,2] Bing Liu,[3] and Guangjin Pan[1,2,*]

[1]CAS Key Laboratory of Regenerative Biology
[2]Guangdong Provincial Key Laboratory of Stem Cell and Regenerative Medicine
South China Institute for Stem Cell Biology and Regenerative Medicine, Guangzhou Institutes of Biomedicine and Health, Chinese Academy of Sciences, Guangzhou 510530, China
[3]Translational Medicine Center for Stem Cells, 307-Ivy Translational Medicine Center, Laboratory of Oncology, Affiliated Hospital of Academy of Military Medical Sciences, Beijing 100071, China
[4]Department of Hematology, Sun-yat Sen University, Guangzhou 510630, China
[5]Co-first author
*Correspondence: pan_guangjin@gibh.ac.cn
http://dx.doi.org/10.1016/j.stemcr.2016.09.008

SUMMARY

The transition from hemogenic endothelial cells (HECs) to hematopoietic stem/progenitor cells (HS/PCs), or endothelial to hematopoietic transition (EHT), is a critical step during hematopoiesis. However, little is known about the molecular determinants of HECs due to the challenge in defining HECs. We report here the generation of *GATA2*$^{w/eGFP}$ reporter in human embryonic stem cells (hESCs) to mark cells expressing *GATA2*, a critical gene for EHT. We show that during differentiation, functional HECs are almost exclusively GATA2/eGFP^{+}. We then constructed a regulatory network for HEC determination and also identified a panel of positive or negative surface markers for discriminating HECs from non-hemogenic ECs. Among them, ITGB3 (CD61) precisely labeled HECs both in hESC differentiation and embryonic day 10 mouse embryos. These results not only identify a reliable marker for defining HECs, but also establish a robust platform for dissecting hematopoiesis in vitro, which might lead to the generation of HSCs in vitro.

INTRODUCTION

Differentiation of functional hematopoietic stem and progenitor cells (HS/PCs) from human pluripotent stem cells (hPSCs) provides a unique source of therapeutic cells for blood diseases and thus generates wide research interests in the field (Daley and Lux, 2014; Liu et al., 2015; Singbrant et al., 2015). Indeed, significant progress have been made on how to drive hPSC differentiation toward different blood lineages (Doulatov et al., 2013; Kennedy et al., 2012; Vodyanik et al., 2005; Wang et al., 2012; Woods et al., 2011). However, HS/PCs derived from hPSCs through current differentiation protocols showed very limited engraftment and hematopoietic reconstitution in vivo (Doulatov et al., 2013; Wang et al., 2005; Woods et al., 2011). These findings indicate that the in vitro conditions for driving blood differentiation do not fully recapitulate the mechanisms of hematopoiesis in vivo. During development, numerous studies using different models such as zebrafish and mouse embryos have shown that hematopoietic stem cells (HSCs) emerge directly from a unique endothelial population, the hemogenic endothelial cells (HECs), through a special process called endothelial to hematopoietic transition (EHT) (Bertrand et al., 2010; Boisset et al., 2010; Tavian et al., 2010). During EHT, cells with endothelium phenotype gradually acquire hematopoietic morphology and characteristics. The EHT process has also been detected during the in vitro blood differentiation of human PSCs (Eilken et al., 2009; Rafii et al., 2013). Therefore, systematic analysis and comparison of the EHT process in vivo and in vitro at the molecular level might aid the generation of functional HS/PCs from hPSCs.

To date, a number of key transcription factors (TFs) and signaling pathways that control EHT have been identified in mouse and zebrafish (Chanda et al., 2013; Clements and Traver, 2013; Kissa and Herbomel, 2010; Wang et al., 2013; Wei et al., 2014). For instance, in mouse embryo, *Runx1* is highly expressed in both HECs and HSCs and plays essential roles in EHT (Chen et al., 2009). GATA2 is another factor that is known to be critical for hematopoiesis (Rodrigues et al., 2012; Vicente et al., 2012). Mouse embryo lacking Gata2 died at an early stage due to the severe anemia (Gao et al., 2013; Lim et al., 2012; Ling et al., 2004; Tsai et al., 1994). Notably, mouse HECs without Gata2 failed to produce long-term repopulating HSCs due to an impaired EHT (de Pater et al., 2013). We have also demonstrated that human embryonic stem cells (hESCs) with *GATA2* deficiency exhibited a reduced EHT during blood

This is an open access article under the CC BY-NC-ND license (http://creativecommons.org/licenses/by-nc-nd/4.0/).

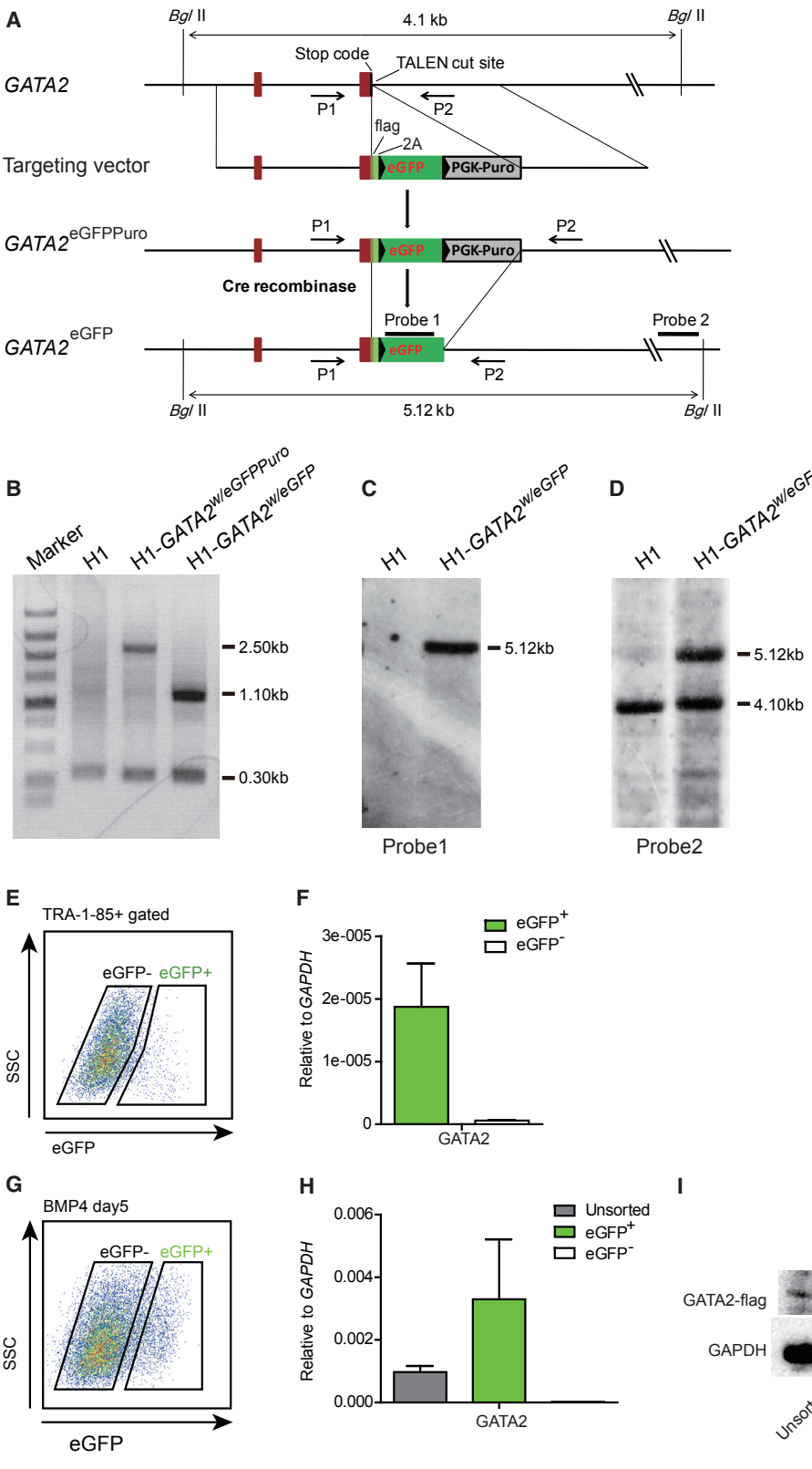

(legend on next page)

differentiation (Huang et al., 2015). These reports suggest that the critical role of GATA2 in regulating EHT is conserved in different species and systems. In addition to the EHT process, TFs also play essential roles in determining the normal function of HS/PCs. For example, overexpression of *Hoxb4* could enhance the engraftment of hematopoietic progenitor cells (HPCs) derived from mouse ESCs (Kyba et al., 2002). However, HOXB4 did not show a similar function in hESC-derived HPCs (Wang et al., 2005), indicating that different TFs need be identified for human cells. Indeed, many other factors such as HOXA9 ERG, RORA, SOX4, and MYB have been tested for promoting engraftment of HS/PCs generated in vitro. However, none of these factors were able to mediate long-term engraftment of these in vitro generated human HS/PCs (Doulatov et al., 2013; Ramos-Mejia et al., 2014; Vanhee et al., 2015). Another approach to generate HS/PCs in vitro is through direct specification of functional HECs into HS/PCs. Indeed, it has been shown that endothelial cells isolated from the aorta gonad mesonephros (AGM) region at embryonic day 10.5 (E10.5) to E11.5 mouse embryos efficiently generated HPCs in vitro (Li et al., 2013). However, how to precisely discriminate the functional HECs from non-hemogenic ECs remains challenging. The inaccessibility of HECs largely hampers the further understanding of their molecular determinants during hematopoiesis.

To further investigate the molecular program involved in HEC determination during human hematopoiesis, we generated a *GATA2/eGFP* reporter in H1 hESCs through gene targeting, referred as *GATA2*$^{w/eGFP}$ hESCs. Based on an hPSC blood differentiation protocol in co-culturing with OP9 (Vodyanik et al., 2005), we show that GATA2/eGFP expression almost exclusively marks the functional HECs with the potential to produce CD34$^+$CD43$^+$ HPCs. We then separated HECs from non-hemogenic ECs in hESC differentiation by cell sorting based on GATA2/eGFP expression. Through further comparative analysis of whole-transcriptome data on GATA2/eGFP$^+$ HECs and GATA2/eGFP$^-$ non-hemogenic ECs, we constructed a regulatory network positive or negative for hemogenic endothelial (HE) determination. Moreover, we identified a list of differentially expressed cell-surface markers between GATA2/eGFP$^+$ HECs and GATA2/eGFP$^-$ ECs. Among them, CD61 precisely labeled functional HECs not only in hESC differentiation but also in yolk sac (YS) or AGM region at E10.0 in mouse embryos. The identification of CD61 provides a reliable marker for accessing and enriching HECs, which might greatly facilitate the understanding of HEC determination both in vivo and in vitro.

RESULTS

Generation of H1 hESC-*GATA2*$^{w/eGFP}$ Cell Line

To target an *eGFP* into *GATA2* locus in human ESCs, we designed a pair of TALENs (transcription activator-like effector nucleases) that could target *GATA2* with high specificity and activity (Cermak et al., 2011; Huang et al., 2015) (Figures S1A–S1D). *GATA2* TALENs along with the linearized *GATA2/eGFP* targeting vector were then electroporated into H1 hESCs for gene editing (Figure 1A). Further through drug selection, the correctly targeted colonies were chosen and verified by PCR with indicated primers (Table S1). Subsequently, the drug-resistant gene was removed with Cre recombinase to obtain the final targeted H1-*GATA2*$^{w/eGFP}$, which was further verified by both PCR (Figure 1B) and Southern bot (Figures 1C and 1D). The final H1-*GATA2*$^{w/eGFP}$ hESCs maintained normal phenotype as do typical hESCs under undifferentiated culture conditions (data not shown). To examine the correlation between *eGFP* and *GATA2* expression, we employed OP9 co-culture for blood differentiation (Vodyanik et al., 2006). As shown in Figure 1E, we detected a significant cell population expressing *eGFP* at day 10 of H1-*GATA2*$^{w/eGFP}$/OP9 co-culture (Figure 1E). The eGFP$^+$ cells showed a much higher level of GATA2 expression while the eGFP$^-$ cells were GATA2

Figure 1. Targeting of eGFP to the *GATA2* Locus in H1 hESCs

(A) Scheme of the *GATA2* locus targeting strategy. Partial *GATA2* locus with *Bgl*II restriction sites is shown (upper) with the targeting vector below it. Homologous recombination aided by TALEN results in the replacement of stop codon with FLAG-2A-eGFP cassette (*GATA2*^{eGFPPuro}). Removal of PGK-Puro cassette with Cre recombinase yields final *GATA2*^{eGFP} locus (lower). PCR primers flanking insertion cassette are labeled with P1 and P2. Probe 1, eGFP probe; Probe 2, 3′ external probe.

(B) PCR analysis (with P1 and P2) of modified H1 hESCs. A 0.3-kb fragment represents the WT *GATA2* allele. The 3.40-kb and 1.1-kb fragments represent the insertion cassette before and after PGK-Puro cassette, respectively.

(C and D) Southern blot analysis of the *GATA2*^{eGFP} H1 hESCs with probes 1 and 2. The heterozygous cell line displays both 4.10-kb and 5.12-kb fragments corresponding to *GATA2* WT and modified allele.

(E) Flow gating strategy of eGFP$^+$ and eGFP$^-$ cells from the TRA-1-85$^+$ fraction at day 10 of H1-*GATA2*$^{w/eGFP}$/OP9 co-culture.

(F) Real-time qPCR analysis of GATA2 expression in the sorted cells as in (E). Error bars represent mean + SEM of the mean of samples from three independent experiments, in this and subsequent figures, unless otherwise indicated.

(G–I) Gating strategy of eGFP$^+$ and eGFP$^-$ cells from BMP4 (50 ng/mL) disposed H1-*GATA2*$^{w/eGFP}$ cells at day 5 (G). Real-time qPCR (H) and western blot (I) (by FLAG antibody) examination of GATA2 expression in each population.

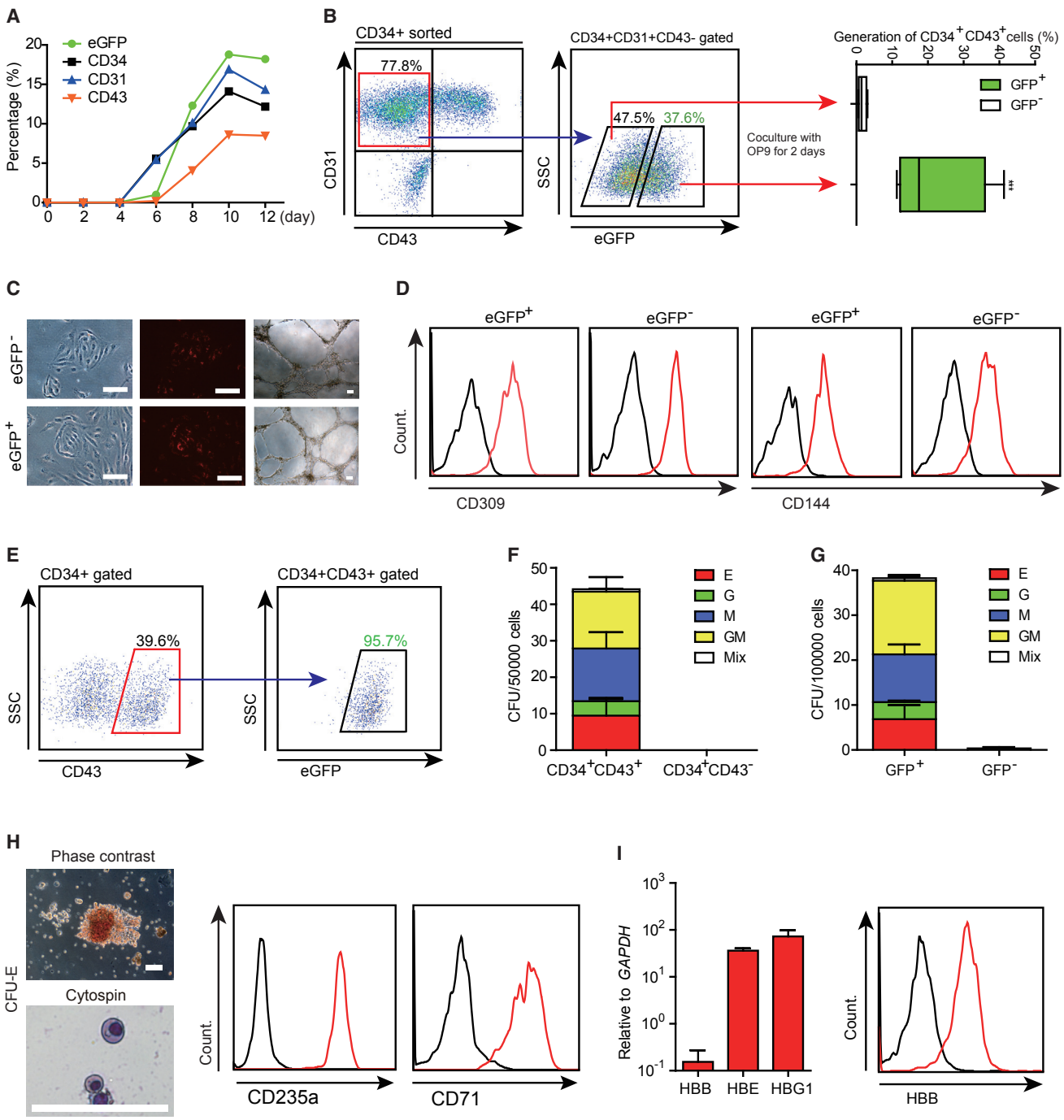

Figure 2. eGFP Expression Marks the HECs and HPCs

(A) FACS analysis of eGFP, CD34, CD31, and CD43 during the H1-*GATA2*$^{w/eGFP}$/OP9 co-culture at indicated time points.

(B) Left and middle: isolation of eGFP$^+$ and eGFP$^-$ cells in CD34$^+$CD31$^+$CD43$^-$ fraction from day 8 of H1-*GATA2*$^{w/eGFP}$/OP9 co-culture; right: FACS analysis of CD34$^+$CD43$^+$ HPC percentage in CD34$^+$ cells. Sorted cells from the middle were co-cultured on OP9 for 2 days before colony-forming assay. Error bars represent mean + SEM of the mean of samples from four independent experiments. Asterisks indicate statistical significance determined by t test: ***$p < 0.001$.

(C) Endothelial potential of eGFP$^+$ and eGFP$^-$ cells from CD34$^+$CD31$^+$CD43$^-$ fraction. Phase contrast, DiI-Ac-LDL uptake, and capillary structure are shown from left to right. Scale bars represent 100 μm in this and subsequent figures unless otherwise indicated.

(D) FACS analysis of CD309 and CD144 expression on the eGFP$^+$ and eGFP$^-$ cells in CD34$^+$CD31$^+$CD43$^-$ fraction.

(legend continued on next page)

negative (Figure 1F), indicating that *eGFP* expression was highly related to *GATA2* expression during differentiation. In addition, we also examined H1-*GATA2*$^{w/eGFP}$ in a bone morphogenetic protein 4 (BMP4)-induced differentiation condition. BMP4 has been reported to induce GATA2 expression (Maeno et al., 1996), hence we examined the GATA2 and eGFP expression in H1-*GATA2*$^{w/eGFP}$ with BMP4 treatment for 5 days. Through both real-time qPCR and western blot, we further confirmed the strict correlation between *eGFP* and *GATA2* expression in another differentiation system (Figures 1G–1I). Altogether, we demonstrated that the eGFP reporter targeted in *GATA2* locus in hESCs could be used to mark the endogenous expression of *GATA2*.

GATA2/eGFP Expression Defines HECs and HPCs in hESC Differentiation

Since GATA2 is a pivotal factor for hematopoiesis, we then analyzed hematopoietic potential on GATA2/eGFP$^+$ and GATA2/eGFP$^-$ populations during blood differentiation. GATA2/eGFP$^+$ cells were detected at the time when CD31$^+$ cells, a previously known HEC population (Nakajima-Takagi et al., 2013) appeared, preceding the formation of CD43$^+$ population, the HPCs identified in hESC differentiation (Vodyanik et al., 2006) (Figure 2A). However, the previously recognized HECs with the phenotype of CD34$^+$CD31$^+$CD43$^-$ contained both GATA2/eGFP$^+$ and GATA2/eGFP$^-$ populations (Figure 2B). Upon sorting and replating onto OP9 stromal cells, only the GATA2/eGFP$^+$ population could further give rise to CD34$^+$CD43$^+$ HPCs (Figure 2B). To further strengthen this finding, we also examined the hematopoietic potential of GATA2/eGFP-positive or -negative cells in a different co-culturing system. Upon co-culturing with another stromal cell, AGM-S3 (Xu et al., 1998), we found again that it was the GATA2/eGFP$^+$, not the GATA2/eGFP$^-$ cells that could efficiently produce HPCs (Figure S2A). In contrast, both GATA2/eGFP$^+$ and GATA2/eGFP$^-$ cells were able to produce monolayer endothelial cells with typical endothelial characteristics such as acetylated low-density lipoprotein (Ac-LDL) uptake and capillary structure formation (Figure 2C). In addition, both GATA2/eGFP$^+$ and GATA2/eGFP$^-$ cells highly express typical endothelial markers such as CD309 and CD144 (Figure 2D). These data demonstrate that at the early stage of blood differentiation, GATA2/eGFP expression marked the functional HECs and could be used to discriminate HECs from non-hemogenic endothelial cells (ECs). Furthermore, we showed that almost all CD34$^+$CD43$^+$ HPCs derived from HECs are also GATA2/eGFP$^+$ (Figure 2E). As expected, these CD34$^+$CD43$^+$GATA2/eGFP$^+$ HPCs were able to form different types of colony-forming unit (CFU) (Figures 2F, S2B, and S2C). Conversely, cell populations sorted by GATA2/eGFP$^+$ from OP9 co-culture exhibited HPC potential in forming different CFUs (Figure 2G). Moreover, we showed that the CFU-erythrocyte derived from GATA2/eGFP$^+$ HECs and HPCs express both embryonic and adult globins, such as HBE, HBG1, and HBB (Figures 2H and 2I). This observation suggests that GATA2/eGFP$^+$ HECs could give rise to HPCs representing both primitive and definitive hematopoietic systems. Taking these data together, we demonstrated that GATA2/eGFP expression labels both HECs and HPCs during blood differentiation of hPSCs.

Molecular Signature of GATA2/eGFP$^+$ HECs

We then analyzed the whole-genome transcriptome on GATA2/eGFP$^+$ HECs and GATA2/eGFP$^-$ ECs during hESC blood differentiation. GATA2/eGFP$^+$ HECs and GATA2/eGFP$^-$ ECs labeled by CD34$^+$CD31$^+$CD43$^-$ were sorted at day 8 of OP9 co-culture and analyzed by RNA sequencing (RNA-seq). Consistent with the phenotype described above, the biological functions of genes upregulated in GATA2/eGFP$^+$ HECs are more related to hematopoiesis (Figure 3A). In contrast, genes upregulated in GATA2/eGFP$^-$ ECs are enriched in endothelium development and angiogenesis (Figure 3A). The critical genes known for normal function of HSC or HSC niche such as ALDH1A1, GFI1, and MYB were enriched in the eGFP$^+$ cells (Ghiaur et al., 2013) (Figure 3C), whereas vital endothelium genes such as SOX17 and NT5E (CD73) were downregulated in the eGFP$^+$ cells (Figure 3B) (Choi et al., 2012; Nakajima-Takagi et al., 2013). Genes known for pan-endothelial, arterial, venous, and lymphatic endothelium were highly expressed in GATA2/eGFP$^-$ ECs (Figure 3D) (Table S3). Notably, some genes related to heart development such as TBX3 (Bakker et al., 2008) and TBX18 (Cai et al., 2008) were also expressed by GATA2-positive cells (Figure 3A). This may be attributed to the elevated expression level of certain GATA factors, GATA6 (Zhao et al., 2008) for example, in the GATA2/eGFP$^+$ population, and these GATA factors are known to be involved and important in cardiac system development. However, factors involved in cardiac development may also be regulated by GATA2 during hematopoiesis, and this needs to be evaluated in future studies.

(E–G) FACS analysis of eGFP expression in CD34$^+$CD43$^+$ cell fraction at day 10 of H1-*GATA2*$^{w/eGFP}$/OP9 co-culture (E). CFU assay of sorted CD34$^+$CD43$^+$, CD34$^+$CD43$^-$ cells (F) and eGFP$^+$, eGFP$^-$ cells (G) at day 10 of H1-*GATA2*$^{w/eGFP}$/OP9 co-culture. E, erythrocyte; G, granulocyte; M, macrophage; GM, G and M; Mix, E, G, and M.

(H) Phase contrast, cytospin, and FACS analysis of CFU-E.

(I) Left: real-time qPCR analysis of HBB, HBE, and HBG1 expression in CFU-E. Right: FACS analysis of HBB expression in CFU-E.

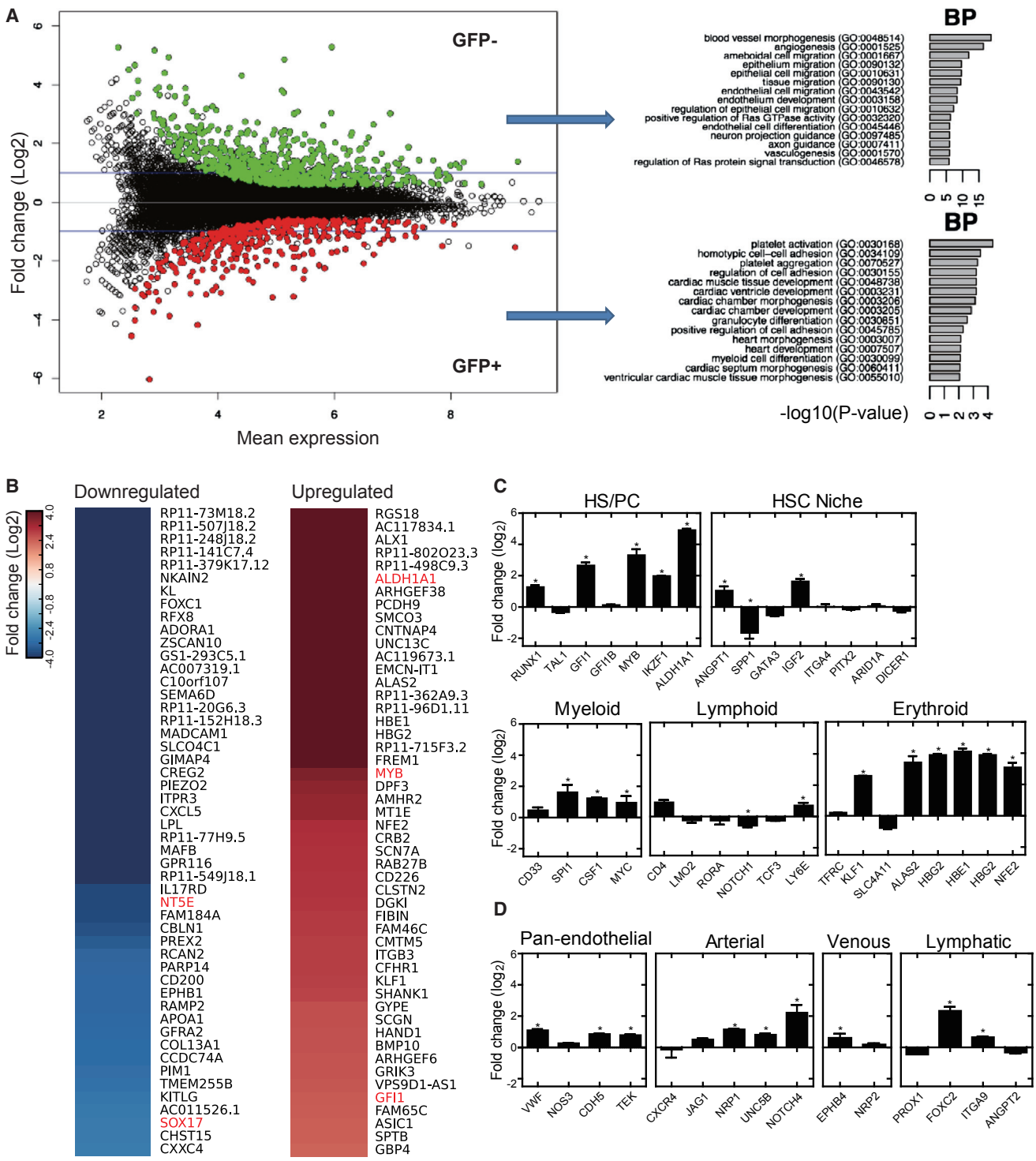

Figure 3. Global Gene Expression Analysis of eGFP$^+$ and eGFP$^-$ Cells in CD34$^+$CD31$^+$CD43$^-$ Fraction by RNA-Seq

(A) Left: MA plot for eGFP$^+$ (n = 2) and eGFP$^-$ (n = 2) cells in CD34$^+$CD31$^+$CD43$^-$ cells from day 8 of H1-*GATA2*$^{w/eGFP}$/OP9 co-culture. The green and red dots represent 708 and 427 upregulated genes in the eGFP$^-$ and eGFP$^+$ cells, respectively ($p < 0.05$). Right: gene ontology analysis of these upregulated genes.

(B) Top 50 genes downregulated and upregulated in the GFP$^+$ cells compared with GFP$^-$ cells ($p < 0.05$). Genes in red have been reported to regulate the EHT process.

(legend continued on next page)

We further identified TFs that were differentially expressed in GATA2/eGFP$^+$ and GATA2/eGFP$^-$ populations. The highly expressed TFs in GATA2/eGFP$^+$ HECs include many well-known critical factors for EHT or HPC function, such as GFI1, RUNX1, MYB, and SPI1. We then sought to investigate whether these TFs form an inter-regulatory network. Based on previously reported protein-protein interaction or gene expression data, we generated an interaction network using the identified GATA2 positively or negatively related TFs (Figure S3B). Notably, 92.1% of the GATA2 negatively related TFs or 83.8% of GATA2 positively related TFs fell into the regulatory interaction network, indicating that these TFs are highly connected and inter-regulated. Such a network would be valuable for further investigations on the molecular mechanism diversifying HECs and non-hemogenic ECs during hematopoiesis.

CD61 Defines Hemogenic Potential Cells during hPSC Differentiation

Identification of reliable cell-surface markers for HECs is critical in enriching well-defined HEC populations for either investigating the mechanism of EHT or developing technologies for generation of HPCs in vitro. We then re-analyzed RNA-seq data and identified differentially expressed surface markers between GATA2/eGFP$^+$ HECs and GATA2/eGFP$^-$ ECs as shown in Figure 4A. The marker lists include many previously known surface markers associated with hematopoietic cells. For example, NT5E (CD73) was upregulated in the GATA2/eGFP$^-$ ECs but not in the GATA2/eGFP$^+$ HECs, which is consistent with previously reported data (Choi et al., 2012). Other reported hematopoietic markers such as CD62P (SELP) (Nkambule et al., 2015) and CD41 (ITGA2B) (Boisset et al., 2013) were upregulated in GATA2/eGFP$^+$ HECs (Figure 4A). We then selected markers that were not extensively analyzed previously and validated them by fluorescence-activated cell sorting (FACS). As shown in Figure 4B, CD226 and CD61 were highly expressed in GATA2/eGFP$^+$ HECs while CD200 preferably marked GATA2/eGFP$^-$ ECs. Among these markers, we were particularly interested in CD61, a member of the integrin family. Integrins are known to be critical in the regulation of cell adhesion, survival, and migration (Schlaepfer et al., 1999). In the mouse system, CD61 has been shown to be enriched in adult HSCs with long-term repopulating potential (Umemoto et al., 2008). However, whether CD61 associates with the HECs preceding the formation of HS/PCs remains unclear. To analyze the hemogenic potential of CD61$^+$ or CD61$^-$ ECs, we sorted and replated them on the OP9 cells, a well-established assay for identification of HECs (Choi et al., 2012). We firstly showed that at day 8 of blood differentiation with OP9 co-culture, CD61$^+$ population is almost all GATA2/eGFP$^+$, while conversely, only part of the GATA2/eGFP$^+$ cells (nearly one-third) are CD61$^+$ (Figure 4C), indicating that CD61 marked a subset of the GATA2/eGFP$^+$ population. However, GATA2/eGFP$^+$CD61$^+$ ECs produced significantly more CD34$^+$CD43$^+$ HPCs than GATA2/eGFP$^+$CD61$^-$ cells upon sorting and replating onto OP9 for co-culture (Figure 4C). These data suggest that the CD61 expression marked the HEC subset in the GATA2/eGFP$^+$ population. We also showed that these CD61$^+$ HECs retain the potential to form a capillary structure of typical ECs and thus are bipotent (Figure 4D). Since the CD61$^-$ cells could also generate a certain number of HPCs (Figure 4C), we asked whether it is possible that some of these CD61$^-$ cells might transit into CD61$^+$ later. Indeed, upon replating onto OP9 cells for 1 day of co-culture, some CD34$^+$CD31$^+$CD43$^-$CD61$^-$ cells transited into CD34$^+$CD31$^+$CD43$^-$CD61$^+$ and then CD34$^+$CD31$^+$CD43$^+$CD61$^+$ HPCs upon differentiation for another day (Figure S4A). In all, these data demonstrate that CD61 is a positive marker for HECs.

Since we have demonstrated the critical role of CD61 in defining HECs using a hESC *GATA2*$^{w/eGFP}$ reporter, we then examined whether it marks HECs in other wild-type (WT) hPSCs. We thus analyzed the blood differentiation of WT hESCs and human induced pluripotent stem cells (hiPSCs), such as H1, H9, and UH1, by OP9 co-culture. We showed that the previous known HEC population defined by CD34$^+$CD31$^+$CD43$^-$ at day 8 of OP9 co-culture contained both CD61$^+$ and CD61$^-$ populations. CD61$^+$ cells from H1, H9, or UH1 gave rise to a significant number of CD34$^+$CD43$^+$ HPCs, while CD61$^-$ cells generated very few CD34$^+$CD43$^+$ HPCs (Figures 4F and 4G). These data demonstrated that CD61 defines a subset population with hemogenic potential in previously identified CD34$^+$CD31$^+$CD43$^-$ endothelium during hPSC blood differentiation. Again, CD61-labeled HECs from WT H1 hESCs are bipotent and can produce typical capillary structure (Figure 4D).

We went on to analyze CD61 expression in CD34$^+$CD43$^+$ HPCs at a later stage during blood differentiation of hPSCs. For the hESC line *GATA2*$^{w/eGFP}$, we showed that almost all CD34$^+$CD43$^+$ HPCs generated by OP9 co-culture were

(C) Fold change of selected genes (associated with the HS/PC, the HSC niche, and myeloid, lymphoid, and erythroid cells) in eGFP$^+$ cells compared with eGFP$^-$ cells. *$p < 0.05$.

(D) Fold change of selected genes associated with pan-endothelial, arterial, venous, and lymphatic cells in eGFP$^-$ cells compared with eGFP$^+$ cells ($q < 0.1$). Error bars represent mean + SEM of the mean of samples from two independent experiments from the RNA-seq data. *$p < 0.05$.

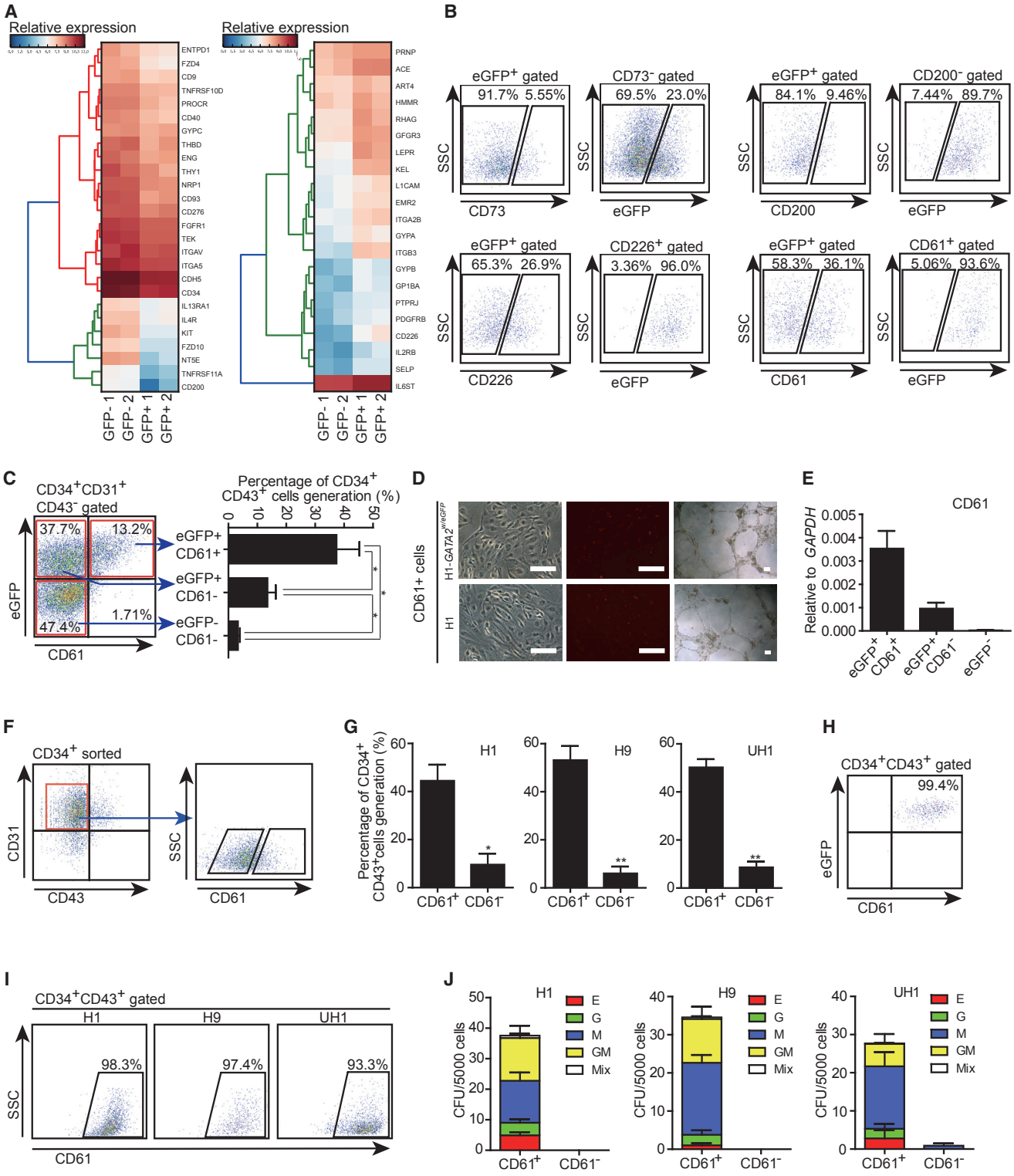

Figure 4. CD61 Expression Marks the HECs and HPCs in hPSC Differentiation

(A) Heatmaps of top differentially expressed cell-surface markers in the eGFP$^-$ and eGFP$^+$ cells in CD34$^+$CD31$^+$CD43$^-$ fraction from day 8 of H1-*GATA2*$^{w/eGFP}$/OP9 co-culture. NT5E in red has been reported to be involved in EHT.

(legend continued on next page)

double positive for GATA2/eGFP and CD61 (Figure 4H). Similarly, for WT hPSC lines H1, H9, and UH1, almost all $CD34^+CD43^+$ HPCs were $CD61^+$ (Figure 4I), indicating that CD61 also served as a marker in defining HPCs. Indeed, we showed that the $CD61^+$ cell population generated a significant number of CFUs while $CD61^-$ cells failed to produce CFUs (Figure 4J). Taking these data together, we demonstrated that CD61 marked both HECs at an early stage and HPCs at a late stage of hPSC differentiation.

CD61 Defines Functional HECs in Mouse Embryo

We then sought to examine whether CD61 defines HECs in vivo in mouse embryo. We firstly examined CD61 expression in a cell population with the EC phenotype defined as $CD31^+CD41^-CD45^-Ter119^-$ from YS and AGM regions at E10.0 (31–34 somite pairs) in mouse embryos. We found that this previously recognized EC population could be fractionated into $CD61^{high}$, $CD61^{low}$, and $CD61^-$ subpopulations. The ECs with different levels of CD61 expression were then sorted and replated onto the OP9 stromal cells for further characterization of hemogenic potential (Figure 5A). Upon OP9 co-culture for 3–4 days, only the $CD61^{low}$ population, regardless of whether from YS or AGM region, could efficiently produce typical hemogenic colonies (up to 6.6 ± 2.4 per embryo equivalent; Figures 5B and 5C). Upon further co-culture (8–9 days), the $CD61^{low}$ fraction, although not other populations, showed robust cell expansion and generation of $CD45^+$ hematopoietic cells (Figures 5B and 5C). These data demonstrate that $CD61^{low}$ marks the subset of HECs in $CD31^+CD41^-CD45^-Ter119^-$ ECs in mouse early embryo. We further showed that $CD61^{low}$ HECs from mouse embryo are bipotent and can produce typical vascular structure (Figures 5D and 5E). In all, we demonstrate that the $CD61^{low}$ cells mark a small subset of functional HECs with bipotency in mouse embryo, and thus could be used to efficiently enrich and access functional HECs (up to a dozen-fold) in vivo for further study.

DISCUSSION

Hematopoiesis is a highly regulated process controlled by the coordination of TFs and diverse signaling pathways. Knowledge of the mechanisms that drive HSC development is critical for generation of functional HSCs in vitro using hPSC differentiation. To date, significant progress has been made in understanding the regulation of HSC development, as well as identification of cell-surface markers defining hematopoietic cells at different developmental stages and regions in animal models (Choi et al., 2012; Kennedy et al., 2012; Wang et al., 2013). However, information on human hematopoiesis remains quite limited due to the inaccessibility of human materials. Hematopoietic differentiation of hESCs in vitro provides a valuable model for understanding human hematopoiesis. It has been known that the in vitro hematopoietic differentiation of hESCs follows the basic principle of the in vivo embryonic hematopoiesis in mouse (Chanda et al., 2013). For example, EHT has been observed during differentiation of hESCs for the generation of HPCs (Rafii et al., 2013). Our previous work also showed that the role of GATA2, a critical factor for mouse hematopoiesis, is conserved in a hESC model, as $GATA2^{-/-}$ hESCs exhibited a significant defect in EHT and then HPC generation (Huang et al., 2015). In the current study, we extended our previous work to generate and analyze the blood differentiation of a hESC $GATA2^{w/eGFP}$ reporter cell line in vitro. We show that both HECs capable of producing HPCs and the generated HPCs are almost exclusively $GATA2/eGFP^+$ cells. These data further highlight the critical role of GATA2 in the regulation of hematopoiesis. It is worth noting that a recent report showed that some HPCs in mice are independent of GATA2, although the HSCs were proved to be exclusively GATA2 expressing (Kaimakis et al., 2016). Our previous work also showed that $GATA2^{-/-}$ hPSC-derived HPCs can produce a certain number of CFUs in vitro (Huang et al., 2015). More detailed analysis of $GATA2^+$ HSCs and $GATA2^-$ HPCs is

(B) Expression pattern of GATA2/eGFP and selected markers (CD73, CD200, CD226, and CD61), in $CD34^+CD31^+CD43^-$ cells at day 8 of hESCs/OP9 co-culture.
(C) $CD34^+CD43^+$ percentage of three sorted cell subpopulations after further 2-day co-culture with OP9. Flow sorting was performed at day 8 of H1-$GATA2^{w/eGFP}$/OP9 co-culture. Asterisks indicate statistical significance determined by t test: *$p < 0.05$.
(D) Endothelial potential of $eGFP^+$ and $eGFP^-$ cells in $CD34^+CD31^+CD43^-$ fraction derived from H1-$GATA2^{w/eGFP}$ and H1/OP9 co-culture. Phase contrast, DiI-Ac-LDL uptake, and capillary structure are shown from left to right.
(E) Real-time qPCR validation of CD61 expression in indicated subpopulations isolated from $CD34^+CD31^+CD43^-$ fraction at day 8 of hESCs/OP9 co-culture.
(F) Gating strategy of $CD61^+$ and $CD61^-$ cell sorting from $CD34^+CD31^+CD43^-$ fraction at day 8 of unmodified hESCs/OP9 co-culture.
(G–I) FACS analysis (G) of $CD34^+CD43^+$ HPC generation (% of $CD34^+$ cells) by H1, H9, and UH1. Cells were sorted as shown above and replated on OP9 for a further 2-day co-culture. Asterisks indicate statistical significance determined by t test: *$p < 0.05$, **$p < 0.01$. FACS analysis of CD61 and eGFP expression in $CD34^+CD43^+$ HPC at day 10 of co-culture of OP9 with H1-$GATA2^{w/eGFP}$ (H) and H1, H9, and UH1 (I).
(J) CFU assay of sorted $CD34^+CD61^+$ and $CD34^+CD61^-$ cells at day 10 of H1, H9, and UH1/OP9 co-culture, respectively.

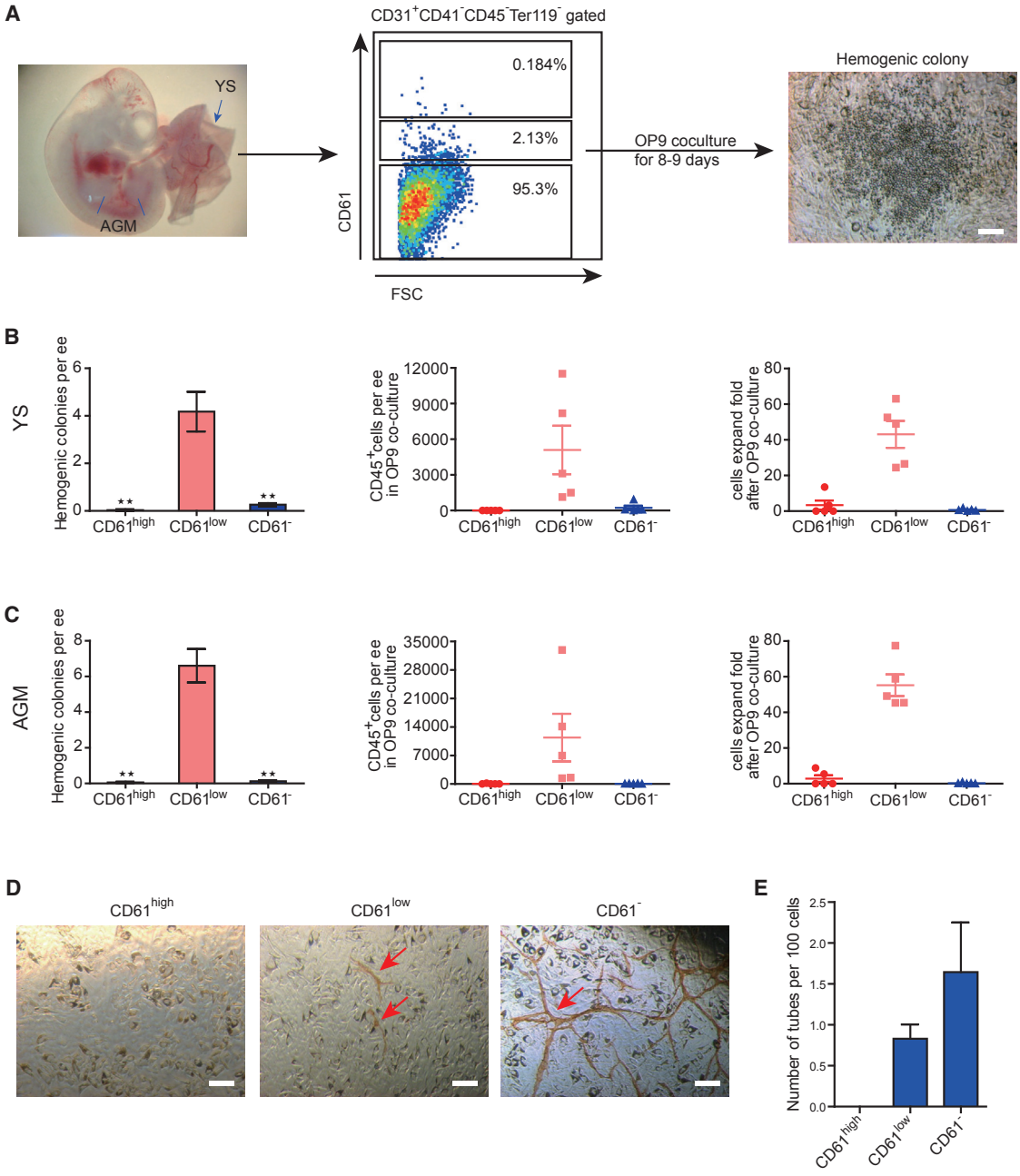

Figure 5. CD61 Labels the HECs in Mouse Embryo

(A) From left to right: picture of YS and AGM at E10 of mouse embryo, FACS analysis of CD61 expression in $CD31^+CD41^-CD45^-Ter119^-$ cells, and picture of typical hemogenic colony formed after co-culture with OP9 stromal cells (original magnification is 5×).

(B and C) From left to right: hemogenic colony formation, $CD45^+$ cell generation, and cell expansion in the co-culture of OP9 with the $CD61^{high}$, $CD61^{low}$, and $CD61^-$ cells in $CD31^+CD41^-CD45^-Ter119^-$ fraction isolated from E10 in YS (B) and AGM (C) regions, respectively. ee, embryo equivalent. Error bars represent mean + SEM of the mean of samples from five independent experiments. Asterisks indicate statistical significance determined by t test: $^{**}p < 0.01$.

(D) Phase contrast of tube formation of the $CD61^{high}$, $CD61^{low}$, and $CD61^-$ cells in $CD31^+CD41^-CD45^-Ter119^-$ fraction. The tubes were stained by anti-CD31 antibody via immunohistochemistry and are indicated by the red arrows.

(E) Statistical analysis of tube formation per 100 cells. Error bars represent mean + SEM of the mean of samples from four independent experiments.

needed in future research to enable full understanding of the role of GATA2 during hematopoiesis.

Nevertheless, given the advantage of GATA2/eGFP as a reporter, we were able to discriminate HECs from non-hemogenic ECs in hESC hematopoietic differentiation. To investigate the molecular determinants for HE, we analyzed and compared the transcriptome of GATA2/eGFP$^+$ HECs and GATA2/eGFP$^-$ ECs derived from hESCs. A panel of TFs that are positive and negative for HECs or ECs were identified in a human model (Figure S3A). Many important TFs for hematopoiesis are relatively conserved between human and mouse. For example, the well-known TFs identified in mouse hematopoietic development, such as GFI1, RUNX1, MYB, and SPI1, are more highly expressed in GATA2/eGFP$^+$ HECs than in GATA2/eGFP$^-$ ECs (Figure S3B). Future work might need to investigate in detail the individual role of each previously unidentified TF in hematopoiesis using both human and mouse models.

Reliable cell-surface markers in defining hematopoietic cells with different potential are valuable in assessing well-defined populations for further investigation. Cell-surface markers are of particular significance for hPSC differentiation, as the in vitro system lacks anatomical and morphological information. To date, a few surface markers have been identified in defining blood cells at different stages of hESC/iPSC differentiation (Choi et al., 2012; Vodyanik et al., 2006). For example, CD43 has been identified as a marker for hPSC-derived HPCs with the potential to form CFUs, thus providing an easy way to isolate HPCs in vitro (Vodyanik et al., 2006). However, defining functional HECs has been complex and challenging due to the limitation of reliable surface markers. Our finding that the HECs are almost exclusively GATA2/eGFP$^+$ allows us to identify reliable surface markers for functional HECs. Indeed, we identified a panel of cell-surface markers that differentially expressed between GATA2/eGFP$^+$ HECs and GATA2/eGFP$^-$ ECs. The lists include some previously identified hematopoietic markers such as CD62P and CD41, and many other unidentified ones. Among them, CD61 is of particular significance as it almost exclusively marked the small portion of HECs capable of producing HPCs in hPSC differentiation. Interestingly, almost all HPCs generated from hPSC-derived HECs are also CD61$^+$. In addition, the CFU-Mix (also referred as GEMM) potential cells were restricted in the CD61^{low} cells in YS of E10 mouse embryo (Figure S5A), indicating that CD61^{low} also labels HPCs in mouse early embryo. In another report, Boisset et al. (2013) also showed that the HSCs with transplantation potential are restricted in the CD61^{low} fraction in E11 AGM and the E11 placenta, while at a later stage, as in the E12 YS and E14 fetal liver, transplantable HSCs were found in both CD61$^-$ and CD61^{low} fractions, indicating that CD61 marks HSCs at the specific stage of mouse embryo.

Another integrin, CD41, was also increased in GATA2/GFP$^+$ HECs. CD41 has been known as a marker to identify HPCs from mouse embryo (Ferkowicz, 2003). However, mouse HECs were defined as CD41$^-$ (CD31$^+$CD41$^-$CD45$^-$Ter119$^-$). Interestingly, CD61 is usually co-expressed with CD41 in many different cell types. However, our findings show that at an early stage of hematopoiesis both in vitro and in vivo, CD61 is expressed independently of CD41 in HECs. Indeed, hematopoietic cells isolated from E8 or E10 mouse embryo exhibited significant differential expression of CD61 and CD41 (Figures S5B and S5C). Similarly, the expressions of CD41 and CD61 are not consistent in hematopoietic cells differentiated from hPSCs in vitro (Figures S4B and S4C). These data indicate that CD61 or CD41 might act independently in certain cell types or stages of hematopoiesis, but their exact roles and timing need to be investigated further. Nonetheless, our finding that CD61 is conservative in defining HECs both in vitro for hPSC differentiation and in vivo for mouse embryo provides valuable information on how to define and access the bipotent HECs. It is noteworthy that the percentage of HECs labeled by CD61 from either YS or AGM is very low, varying between 2% and 10% of previously recognized ECs (Figure 5A). Therefore, the identification of CD61 would allow dozen-fold enrichment for HECs and would greatly facilitate future research in understanding the mechanisms of HE determination and HSC generation both in vitro and in vivo.

EXPERIMENTAL PROCEDURES

All experiments were carried out in accordance with the guidelines of the Human Subject Research Ethics Committee at Guangzhou Institutes of Biomedicine and Health (GIBH), Chinese Academy of Sciences (CAS), and all experimental protocols were approved by the committee. Formal informed consent was obtained from all subjects.

All animal experiments were carried out in accordance with the Guide for the Care and Use of Laboratory Animals instructed by the Institutional Animal Care and Use Committee of Guangzhou Institutes of Biomedicine and Health (IACUC-GIBH) and all protocols were approved by the committee.

TALEN Targeting

The binding and cutting sites of GATA2 knockin TALENs are illustrated in Figure S1, and the TALENs were designed as previously described (Huang et al., 2015). For donor construction, left and right homology arms were cloned from genomic DNA of H1 cell line about 1 kb upstream and downstream of the stop code, respectively. A FLAG-2A-eGFP-loxP-PGK-puromycin-loxP cassette was further inserted into the homology arms in the vector pUC57. For targeting, constructed vector was initially linearized by *Eco*RI,

then 1 μg of the linearized vector was electroporated into 1 × 10^6 H1 cells with 2.5 μg of each TALEN plasmid. After the transfection, cells were seeded on Matrigel-coated 6-well plates in the presence of 10 μM Y-27632 (Sigma). Puromycin (0.5 μg/mL, Sigma) was added to the medium to select positive clones 2 or 3 days later. Drug-resistant clones were picked out and genomic DNA of these clones was used for PCR verification of successful targeting. After the verification, the targeted clones were expanded and further transfected with 400 ng of Cre recombinase for every 1 × 10^6 cells to remove the *loxP* flanked PGK-puromycin cassette, followed by seeding in a single-cell state in the presence of Y-27632. When the clones grew up, they were picked for further verifications by genomic PCR and Southern blot.

The GFP reporter assay was performed as previously reported (Huang et al., 2015). In brief, the GFP reporter was inserted with the WT or mutant sequence of the TALENs binding and cutting sites. The reporter was then electroporated into the 293T cells with the TALENs for test. After 48 hr, the cells were digested and examined for GFP fluorescence by FACS.

PCR and Southern Blot Verification

PCR reactions were performed with KOD-Plus enzyme (Toyobo) according to the manufacturer's instructions. For each reaction, 50–100 ng of genomic DNA templates were used. PCR primers P1 and P2 (shown in Figure 1A) were designed to amplify 2.50-kb or 1.10-kb products. The 2.50-kb product was obtained from cell line with the *loxP* flanked PGK-puromycin cassette. After removal of the cassette, the 1.10-kb product was produced as illustrated in Figure 1B. For Southern blot, the reactions were carried out according to the manuals of DIG High Prime DNA Labeling and Detection Starter Kit II (Roche). Specifically, genomic DNA was digested by *Bgl*II endonuclease, and probes about 1 kb in length were synthesized by PCR reaction. The eGFP probe (probe 1) was used to verify the integration of a single copy of eGFP sequence in the genome, and the 3′ external probe (probe 2) was used to identify the insertion in the TALEN cutting site as designed. All primers are listed in Table S1.

hPSC Culture and Differentiation in Co-culture

The procedures of hESC (H1 and H9) and hiPSC (UH1) culture, and OP9-based hematopoietic differentiation were carried out as described previously (Huang et al., 2015). In particular, gene targeting was performed at passage 38 of the H1 ESC line. In addition, $CD34^+CD31^+CD43^-$ HECs at day 8 of hESC/OP9 co-culture and $CD34^+CD43^+$ HPCs at day 10 of hESCs/OP9 co-culture were sorted for further analysis. Furthermore, for assessment of hemogenic potential of HECs or HE subpopulation, cells sorted at day 8 of differentiation were replated onto OP9 or AGM-S3 stromal cells for 1 or 2 further days of co-culture before analysis.

FACS Analysis and Cell Sorting

The detailed procedure is presented in Supplemental Experimental Procedures.

CFU Assay

CFU assay of hESC-derived HPCs was conducted following the manufacturer's protocol H4435 (STEMCELL). For CFU assay of mouse scored cells, cells were plated in 0.9% methylcellulose-based medium supplemented with 15% fetal bovine serum, 2 mM glutamine, 100 U/mL penicillin-streptomycin, 5% protein-free hybridoma medium II, 200 mg/mL iron-saturated holo-transferrin, 1% BSA, 0.45 mM monothioglycerol, 100 ng/mL recombinant murine stem cell factor (PeproTech), 10 ng/mL recombinant murine interleukin-3, 10 ng/mL recombinant human interleukin-6, and 3 U/mL human erythropoietin. Colonies were scored based on the morphological criteria.

Real-Time qPCR

The detailed procedure is presented in Supplemental Experimental Procedures.

RNA-Seq

RNA-seq and subsequent data analysis were conducted as described by Huang et al. (2015). In brief, total RNA was isolated with a Direct-zol RNA MiniPrep kit (Zymo Research) and sequencing libraries was prepared with a TruSeq RNA Sample Prep Kit (Illumina) following the manufacturer's protocol. The samples were run on an MiSeq system with MiSeq Reagent Kits v2 (50 cycles) (Illumina). In particular, RNA-seq data were processed essentially as described by Hutchins et al. (2015), reads were aligned to an index generated from the Ensembl transcriptome version 74 (hg19) using RSEM (v1.2.19), Bowtie2 (v2.2.5), and normalized with EDASeq (v2.2.0). Gene expression is expressed as "normalized tag count." A threshold of at least 20 normalized tags in any condition was used to filter lowly expressed transcripts. Differential expression was performed using DESeq2 (v1.8.1) and genes were considered significant if they had a Benjamini-Hochberg corrected p value (q value) <0.1 and had a fold-change > 1.5. Gene ontology was performed using goseq (v1.20.0). Other analyses were performed using glbase (Hutchins et al., 2014).

Endothelial Cell Culture and Assays

Endothelial cell-related assays, including endothelial cell culture, DiI-Ac-LDL uptake, and capillary structure formation, were performed as described previously (Huang et al., 2015). In brief, the $eGFP^+$ and $eGFP^-$ cells in $CD34^+CD31^+CD43^-$ cells were sorted from day 8 of H1-*GATA2*$^{w/eGFP}$/OP9 co-culture. Specifically, the DiI-Ac-LDL uptake assay was performed as per the manual's instructions. FACS-sorted $CD61^{high}$, $CD61^{low}$, and $CD61^-$ cells in the $CD31^+CD41^-CD45^-Ter119^-$ fraction were cultured on an OP9 stromal cell layer to detect the endothelial cell colony formation in the presence of 100 ng/mL vascular endothelial growth factor. After 7 days, cultured cells were fixed with 4% paraformaldehyde and the forming capacity of endothelial tubules was assessed by immunostaining with anti-CD31 antibody (BD Pharmingen). Immunohistochemistry was performed as described previously (Lan et al., 2007).

Mice and YS/AGM Cell Preparation

The detailed procedure is presented in Supplemental Experimental Procedures.

Co-culture of YS and AGM Cell with OP9

The detailed procedure is presented in Supplemental Experimental Procedures.

Western Blot

The detailed procedure is presented in Supplemental Experimental Procedures.

ACCESSION NUMBERS

The accession number of the RNA-seq data reported in this paper is GEO: GSE74041.

SUPPLEMENTAL INFORMATION

Supplemental Information includes Supplemental Experimental Procedures, five figures, and three tables and can be found with this article online at http://dx.doi.org/10.1016/j.stemcr.2016.09.008.

AUTHOR CONTRIBUTIONS

K.H. initiated the study, designed and performed the experiments, and analyzed the data; J.G. performed the mouse embryo assay and analyzed the data; J.D. directed the study, revised the manuscript, and performed the RNA-seq with Q.C.; N.M. performed gene targeting with K.H.; A.P.H. and Z.Y., analyzed the RNA-seq data; Y.Z., Y.L., and W.W. assisted with the RNA extraction and real-time qPCR analysis; Y.Z., P.W., Y.Z., and T.Z. assisted with the FACS analysis; J.Z. performed the teratoma assay; Y.S. performed the western blot; X.L. assisted with the hematopoietic differentiation; B.L., J.L., J.W., and D.P. directed the study and revised the manuscript; B.L. instructed the mouse embryo assay and revised the manuscript; G.P. conceived and supervised the whole study and wrote the manuscript.

ACKNOWLEDGMENTS

We thank Dr. Duanqing Pei for the constructive comments and members of the laboratory in GIBH for their kind help. We thank Dr. Edouard G. Stanley for helpful discussions regarding gene targeting. This work was supported by the National Basic Research Program of China, 973 Program of China, (2012CB966503, 2015CB964902, 2015CB964901); the National Natural Science Foundation of China, (31500948, 81200337); Cooperation Grant of Natural Science Foundation of Guangdong Province, (2014A030312012); the Science and Information Technology of Guangzhou Key Project, (201508020258); the Youth Innovation Promotion Association of the Chinese Academy of Sciences, (2015293, 2014327); the Frontier and key technology innovation special grant from the Department of Science and Technology of Guangdong province, (2014B020225005, 2014B020225006, 2016B030229008); International Science & Technology Cooperation Program of China (2014DFA30180); Strategic Priority Research Program of the Chinese Academy of Sciences (XDA01020202); "Hundred Talents Program" of the Chinese Academy of Science (to G.P.).

Received: February 29, 2016
Revised: September 16, 2016
Accepted: September 16, 2016
Published: October 13, 2016

REFERENCES

Bakker, M.L., Boukens, B.J., Mommersteeg, M.T., Brons, J.F., Wakker, V., Moorman, A.F., and Christoffels, V.M. (2008). Transcription factor Tbx3 is required for the specification of the atrioventricular conduction system. Circ. Res. *102*, 1340–1349.

Bertrand, J.Y., Chi, N.C., Santoso, B., Teng, S., Stainier, D.Y., and Traver, D. (2010). Haematopoietic stem cells derive directly from aortic endothelium during development. Nature *464*, 108–111.

Boisset, J.C., van Cappellen, W., Andrieu-Soler, C., Galjart, N., Dzierzak, E., and Robin, C. (2010). In vivo imaging of haematopoietic cells emerging from the mouse aortic endothelium. Nature *464*, 116–120.

Boisset, J.C., Clapes, T., Van Der Linden, R., Dzierzak, E., and Robin, C. (2013). Integrin alphaIIb (CD41) plays a role in the maintenance of hematopoietic stem cell activity in the mouse embryonic aorta. Biol. Open *2*, 525–532.

Cai, C.L., Martin, J.C., Sun, Y.F., Cui, L., Wang, L.C., Ouyang, K., Yang, L., Bu, L., Liang, X.Q., Zhang, X.X., et al. (2008). A myocardial lineage derives from Tbx18 epicardial cells. Nature *454*, 104–108.

Cermak, T., Doyle, E.L., Christian, M., Wang, L., Zhang, Y., Schmidt, C., Baller, J.A., Somia, N.V., Bogdanove, A.J., and Voytas, D.F. (2011). Efficient design and assembly of custom TALEN and other TAL effector-based constructs for DNA targeting. Nucleic Acids Res. *39*, e82.

Chanda, B., Ditadi, A., Iscove, N.N., and Keller, G. (2013). Retinoic acid signaling is essential for embryonic hematopoietic stem cell development. Cell *155*, 215–227.

Chen, M.J., Yokomizo, T., Zeigler, B.M., Dzierzak, E., and Speck, N.A. (2009). Runx1 is required for the endothelial to haematopoietic cell transition but not thereafter. Nature *457*, 887–891.

Choi, K.D., Vodyanik, M.A., Togarrati, P.P., Suknuntha, K., Kumar, A., Samarjeet, F., Probasco, M.D., Tian, S., Stewart, R., Thomson, J.A., et al. (2012). Identification of the hemogenic endothelial progenitor and its direct precursor in human pluripotent stem cell differentiation cultures. Cell Rep. *2*, 553–567.

Clements, W.K., and Traver, D. (2013). Signalling pathways that control vertebrate haematopoietic stem cell specification. Nat. Rev. Immunol. *13*, 336–348.

Daley, G.Q., and Lux, S.E. (2014). Deriving blood stem cells from pluripotent stem cells for research and therapy. Best. Pract. Res. Clin. Haematol. *27*, 293–297.

de Pater, E., Kaimakis, P., Vink, C.S., Yokomizo, T., Yamada-Inagawa, T., van der Linden, R., Kartalaei, P.S., Camper, S.A., Speck, N., and Dzierzak, E. (2013). Gata2 is required for HSC generation and survival. J. Exp. Med. *210*, 2843–2850.

Doulatov, S., Vo, L.T., Chou, S.S., Kim, P.G., Arora, N., Li, H., Hadland, B.K., Bernstein, I.D., Collins, J.J., Zon, L.I., et al. (2013). Induction of multipotential hematopoietic progenitors from human pluripotent stem cells via respecification of lineage-restricted precursors. Cell Stem Cell *13*, 459–470.

Eilken, H.M., Nishikawa, S.I., and Schroeder, T. (2009). Continuous single-cell imaging of blood generation from haemogenic endothelium. Nature *457*, 896–900.

Ferkowicz, M.J. (2003). CD41 expression defines the onset of primitive and definitive hematopoiesis in the murine embryo. Development *130*, 4393–4403.

Gao, X., Johnson, K.D., Chang, Y.I., Boyer, M.E., Dewey, C.N., Zhang, J., and Bresnick, E.H. (2013). Gata2 cis-element is required for hematopoietic stem cell generation in the mammalian embryo. J. Exp. Med. *210*, 2833–2842.

Ghiaur, G., Yegnasubramanian, S., Perkins, B., Gucwa, J.L., Gerber, J.M., and Jones, R.J. (2013). Regulation of human hematopoietic stem cell self-renewal by the microenvironment's control of retinoic acid signaling. Proc. Natl. Acad. Sci. USA *110*, 16121–16126.

Huang, K., Du, J., Ma, N., Liu, J., Wu, P., Dong, X., Meng, M., Wang, W., Chen, X., Shi, X., et al. (2015). GATA2(-/-) human ESCs undergo attenuated endothelial to hematopoietic transition and thereafter granulocyte commitment. Cell Regen. (Lond) *4*, 4.

Hutchins, A.P., Jauch, R., Dyla, M., and Miranda-Saavedra, D. (2014). glbase: a framework for combining, analyzing and displaying heterogeneous genomic and high-throughput sequencing data. Cell Regen. (Lond) *3*, 1.

Hutchins, A.P., Takahashi, Y., and Miranda-Saavedra, D. (2015). Genomic analysis of LPS-stimulated myeloid cells identifies a common pro-inflammatory response but divergent IL-10 anti-inflammatory responses. Sci. Rep. *5*, 9100.

Kaimakis, P., de Pater, E., Eich, C., Kartalaei, P.S., Kauts, M.L., Vink, C.S., van der Linden, R., Jaegle, M., Yokomizo, T., Meijer, D., et al. (2016). Functional and molecular characterization of mouse Gata2-independent hematopoietic progenitors. Blood *127*, 1426–1437.

Kennedy, M., Awong, G., Sturgeon, C.M., Ditadi, A., Lamotte-Mohs, R., Zuniga-Pflucker, J.C., and Keller, G. (2012). T lymphocyte potential marks the emergence of definitive hematopoietic progenitors in human pluripotent stem cell differentiation cultures. Cell Rep. *2*, 1722–1735.

Kissa, K., and Herbomel, P. (2010). Blood stem cells emerge from aortic endothelium by a novel type of cell transition. Nature *464*, 112–115.

Kyba, M., Perlingeiro, R.C.R., and Daley, G.Q. (2002). HoxB4 confers definitive lymphoid-myeloid engraftment potential on embryonic stem cell and yolk sac hematopoietic progenitors. Cell *109*, 29–37.

Lan, Y., Liu, B., Yao, H.Y., Li, F.F., Weng, T.J., Yang, G., Li, W.L., Cheng, X., Mao, N., and Yang, X. (2007). Essential role of endothelial Smad4 in vascular remodeling and integrity. Mol. Cell. Biol. *27*, 7683–7692.

Li, Z., Zhou, F., Chen, D., He, W., Ni, Y., Luo, L., and Liu, B. (2013). Generation of hematopoietic stem cells from purified embryonic endothelial cells by a simple and efficient strategy. J. Genet. Genomics *40*, 557–563.

Lim, K.C., Hosoya, T., Brandt, W., Ku, C.J., Hosoya-Ohmura, S., Camper, S.A., Yamamoto, M., and Engel, J.D. (2012). Conditional Gata2 inactivation results in HSC loss and lymphatic mispatterning. J. Clin. Invest. *122*, 3705–3717.

Ling, K.W., Ottersbach, K., van Hamburg, J.P., Oziemlak, A., Tsai, F.Y., Orkin, S.H., Ploemacher, R., Hendricks, R.W., and Dzierzak, E. (2004). GATA-2 plays two functionally distinct roles during the ontogeny of hematopoietic stem cells. J. Exp. Med. *200*, 871–882.

Liu, S.Q., Xu, Y.L., Zhou, Z.J., Feng, B., and Huang, H. (2015). Progress and challenges in generating functional hematopoietic stem/progenitor cells from human pluripotent stem cells. Cytotherapy *17*, 344–358.

Maeno, M., Mead, P.E., Kelley, C., Xu, R.H., Kung, H.F., Suzuki, A., Ueno, N., and Zon, L.I. (1996). The role of BMP-4 and GATA-2 in the induction and differentiation of hematopoietic mesoderm in Xenopus laevis. Blood *88*, 1965–1972.

Nakajima-Takagi, Y., Osawa, M., Oshima, M., Takagi, H., Miyagi, S., Endoh, M., Endo, T.A., Takayama, N., Eto, K., Toyoda, T., et al. (2013). Role of SOX17 in hematopoietic development from human embryonic stem cells. Blood *121*, 447–458.

Nkambule, B.B., Davison, G., and Ipp, H. (2015). Platelet leukocyte aggregates and markers of platelet aggregation, immune activation and disease progression in HIV infected treatment naive asymptomatic individuals. J. Thromb. Thrombolysis *40*, 458–467.

Rafii, S., Kloss, C.C., Butler, J.M., Ginsberg, M., Gars, E., Lis, R., Zhan, Q.S., Josipovic, P., Ding, B.S., Xiang, J., et al. (2013). Human ESC-derived hemogenic endothelial cells undergo distinct waves of endothelial to hematopoietic transition. Blood *121*, 770–780.

Ramos-Mejia, V., Navarro-Montero, O., Ayllon, V., Bueno, C., Romero, T., Real, P.J., and Menendez, P. (2014). HOXA9 promotes hematopoietic commitment of human embryonic stem cells. Blood *124*, 3065–3075.

Rodrigues, N.P., Tipping, A.J., Wang, Z.K., and Enver, T. (2012). GATA-2 mediated regulation of normal hematopoietic stem/progenitor cell function, myelodysplasia and myeloid leukemia. Int. J. Biochem. Cell Biol. *44*, 457–460.

Schlaepfer, D.D., Hauck, C.R., and Sieg, D.J. (1999). Signaling through focal adhesion kinase. Prog. Biophys. Mol. Biol. *71*, 435–478.

Singbrant, S., van Galen, P., Lucas, D., Challen, G., Rossi, D.J., and Daley, G.Q. (2015). Two new routes to make blood: hematopoietic specification from pluripotent cell lines versus reprogramming of somatic cells. Exp. Hematol. *43*, 756–759.

Tavian, M., Biasch, K., Sinka, L., Vallet, J., and Peault, B. (2010). Embryonic origin of human hematopoiesis. Int. J. Dev. Biol. *54*, 1061–1065.

Tsai, F.Y., Keller, G., Kuo, F.C., Weiss, M., Chen, J.Z., Rosenblatt, M., Alt, F.W., and Orkin, S.H. (1994). An early hematopoietic defect in mice lacking the transcription factor gata-2. Nature *371*, 221–226.

Umemoto, T., Yamato, M., Shiratsuchi, Y., Terasawa, M., Yang, J., Nishida, K., Kobayashi, Y., and Okano, T. (2008). CD61 enriches long-term repopulating hematopoietic stem cells. Biochem. Biophys. Res. Commun. *365*, 176–182.

Vanhee, S., De Mulder, K., Van Caeneghem, Y., Verstichel, G., Van Roy, N., Menten, B., Velghe, I., Philippe, J., De Bleser, D., Lambrecht, B.N., et al. (2015). In vitro human embryonic stem cell hematopoiesis mimics MYB-independent yolk sac hematopoiesis. Haematologica *100*, 157–166.

Vicente, C., Conchillo, A., Garcia-Sanchez, M.A., and Odero, M.D. (2012). The role of the GATA2 transcription factor in normal and malignant hematopoiesis. Crit. Rev. Oncol. Hematol. *82*, 1–17.

Vodyanik, M.A., Bork, J.A., Thomson, J.A., and Slukvin, I.I. (2005). Human embryonic stem cell-derived CD34+ cells: efficient production in the coculture with OP9 stromal cells and analysis of lymphohematopoietic potential. Blood *105*, 617–626.

Vodyanik, M.A., Thomson, J.A., and Slukvin, I.I. (2006). Leukosialin (CD43) defines hematopoietic progenitors in human embryonic stem cell differentiation cultures. Blood *108*, 2095–2105.

Wang, L., Menendez, P., Shojaei, F., Li, L., Mazurier, F., Dick, J.E., Cerdan, C., Levac, K., and Bhatia, M. (2005). Generation of hematopoietic repopulating cells from human embryonic stem cells independent of ectopic HOXB4 expression. J. Exp. Med. *201*, 1603–1614.

Wang, C., Tang, X., Sun, X., Miao, Z., Lv, Y., Yang, Y., Zhang, H., Zhang, P., Liu, Y., Du, L., et al. (2012). TGFbeta inhibition enhances the generation of hematopoietic progenitors from human ES cell-derived hemogenic endothelial cells using a stepwise strategy. Cell Res. *22*, 194–207.

Wang, L., Liu, T.H., Xu, L.J., Gao, Y., Wei, Y.L., Duan, C.W., Chen, G.Q., Lin, S., Patient, R., Zhang, B., et al. (2013). Fev regulates hematopoietic stem cell development via ERK signaling. Blood *122*, 367–375.

Wei, Y.L., Ma, D.Y., Gao, Y., Zhang, C.X., Wang, L., and Liu, F. (2014). Ncor2 is required for hematopoietic stem cell emergence by inhibiting Fos signaling in zebrafish. Blood *124*, 1578–1585.

Woods, N.B., Parker, A.S., Moraghebi, R., Lutz, M.K., Firth, A.L., Brennand, K.J., Berggren, W.T., Raya, A., Belmonte, J.C., Gage, F.H., et al. (2011). Brief report: efficient generation of hematopoietic precursors and progenitors from human pluripotent stem cell lines. Stem Cells *29*, 1158–1164.

Xu, M.J., Tsuji, K., Ueda, T., Mukouyama, Y., Hara, T., Yang, F.C., Ebihara, Y., Matsuoka, S., Manabe, A., Kikuchi, A., et al. (1998). Stimulation of mouse and human primitive hematopoiesis by murine embryonic aorta-gonad-mesonephros-derived stromal cell lines. Blood *92*, 2032–2040.

Zhao, R., Watt, A.J., Battle, M.A., Li, J., Bondow, B.J., and Duncan, S.A. (2008). Loss of both GATA4 and GATA6 blocks cardiac myocyte differentiation and results in acardia in mice. Dev. Biol. *317*, 614–619.